37 P.

5793

dS TT 636128

SIMULATION AND ANALYSIS OF A GEOPOTENTIAL RESEARCH MISSION

SEMI-ANNUAL STATUS REPORT
GRANT NAG5-528

Principal Investigator:

B. E. Schutz
The University of Texas at Austin
Center for Space Research
Austin, Texas 78712
(512) 471-4267

JUNE 1986

SUMMARY

The major activities of the past six-month period were as follows:

- Preparation of a paper entitled, *Simulation and Analysis of a Geopotential Research Mission.* The paper is given in Appendix A and will be submitted for journal publication.
- Preparation of magnetic tapes containing the data created for the GRM simulation. The format of the tape is given in Appendix B.
- Initial preparation for follow-on studies.

On May 8, 1986, tapes containing the simulated data were delivered to Frank Lerch (GSFC) and Carl Wagner (NGS). On May 15, a tape was mailed to Dr. S. Boze (Applied Sciences Analytics).

A paper entitled, *Simulation of a Geopotential Research Mission (GRM)*, will be presented at the COSPAR meeting in Toulouse, France, on July 4, 1986.

APPENDIX A

SIMULATION OF A GEOPOTENTIAL RESEACH MISSION FOR GRAVITY STUDIES

SIMULATION OF A GEOPOTENTIAL RESEARCH MISSION FOR GRAVITY STUDIES

B. E. Schutz, B. D. Tapley, J. B. Lundberg and P. Halamek
Center for Space Research
The University of Texas at Austin
Austin, Texas 78712

ABSTRACT

A computer simulation has been performed for a Geopotential Research Mission (GRM) to enable study of the gravitational sensitivity of the range-rate measurement between two satellites and to provide a set of simulated measurements to assist in the evaluation of techniques developed for the determination of the gravity field. The simulation, identified as SGRM 8511, was conducted with two satellites in near circular, frozen orbits at 160 km altitude and separated by 300 km. High precision numerical integration of the polar orbits was used with a gravitational field complete to degree and order 180 coefficients and to degree 300 in orders 0 to 10. The set of simulated data for a mission duration of about 32 days was generated on a Cray X-MP computer. The characteristics of the simulation and the nature of the results are described in this report.

INTRODUCTION

The determination of the earth's gravity field by the Geopotential Research Mission (GRM) will be achieved using two satellites moving in essentially coincident orbit planes but separated by 100 to 600 km. Precise measurements of the range-rate between the two polar inclination satellites would provide a data set from which the gravity information would be extracted. With a range-rate measurement precision of one micron per second or better and an orbit altitude of 160 km, it is expected that the data set would provide resolutions of at least 1-2 mgal in gravity anomalies, 5-10 cm in geoid height, and 100 km spatially [*Taylor et al.*, 1984]. Applications of this mission to geophysics, geodesy and oceanography are discussed by the *National Research Council* [1979] and *Keating et*

al., [1986].

For the desired resolution, it is essential that the gravity field be recovered to a high degree and order in the spherical harmonic representation or other representations. However, use of the range-rate data in the procedures commonly used in satellite geodesy for gravity field determinations (e.g., *Lerch et al.*, 1985) would result in the need to solve very large systems of equations. For example, a degree and order 180 (or 180×180) field would require the inversion of a full, symmetric matrix of dimension exceeding 32,000. The computational effort associated with such an inversion would be significant, even for current supercomputers. Although supercomputers are expected to be available by 1990 with physical memory storage exceeding 1 billion 64-bit words, thereby enabling storage of a complete 32000×32000 matrix in main memory, the computational problems associated with such an inversion are still significant.

Alternate procedures have been proposed to circumvent the need for inversion of a very large matrix. These procedures include those proposed by *Colombo* [1984], *Kaula* [1983], *Wagner* [1983], and others. While these procedures are promising, none have been tested on a set of simulated data derived from the solution of dynamically consistent equations of motion.

The goal of the investigation described in this report was the creation of a set of simulated range-rate data that could be used for studies of techniques applicable to recovery of the gravity field from GRM range-rate data. The simulation model, the supporting studies of the computational accuracy, and the characteristics of the resulting simulated data are discussed in the following sections.

GRM DESCRIPTION

The 160 km altitude proposed for the GRM results in significant forces acting on each spacecraft due to atmospheric resistance. Past experience has demonstrated difficulty in adequately modeling this force, however, its signature is very similar to that produced by various gravitational coefficients. As a consequence, it is essential that the force be directly removed or measured. The

GRM uses a "drag-free" concept, as described by *Taylor et al.* [1984] and *Keating et al.*, [1986], to effectively remove the effects of all nongravitational forces, including solar and earth radiation pressure as well as atmospheric forces.

The range-rate system of the GRM operates at 91 GHz and 42 GHz to enable removal of the ionospheric effects on the measurement. To meet the mission objectives, it is expected that the relative velocity variations must be measured to an accuracy of 2.5 microns per second every four seconds. Furthermore, it is anticipated that the range between the two spacecraft would be adjusted between 150 and 550 km during the six-month mission duration launched from the shuttle orbiter. The 2600-2800 kg spacecraft would be tracked by the Defense Mapping Agency TRANET doppler system.

The GRM measurement is sensitive to gravitational effects produced by a variety of sources, including temporal variations. Compared to higher altitude satellites at typical geodetic altitude of 1000 km, the influence of solid earth and ocean tide effects will be enhanced, however, the direct luni-solar gravitational effects will be diminished.

SIMULATION DESCRIPTION

A complete simulation of the GRM is desirable to enable the testing of techniques for determining the gravity field from the range-rate signal in a realistic environment. However, the wide range of forces and kinematical effects noted in the preceding section that should be included in the simulation will complicate the studies directed toward the technique tests.

In order to enhance the primary gravitational signal and offer the recovery techniques a set of simulated data that is not complicated by signals from other sources, it was concluded that the initial simulation should exhibit only the primary features of the actual GRM. As a consequence, the temporal variations in the gravity field and direct luni-solar forces were not included. It was also assumed that the spacecraft moved in an environment free of nongravitational forces; however,

specific modeling of the thrusting associated with the drag compensation mechanism was not included. Furthermore, the effects of precession, nutation, polar motion and UT1 variations were not included. The specific model characteristics for the simulation are shown in Table 1.

Since the specific orbit characteristics for GRM have not been selected, the adopted orbits resulted from discussions within the International Association of Geodesy Special Study Group 2.83, chaired by Dr. R. Rummel, Delft University. Although the planned mission would use different separation distances over a mission duration of six months, a simulation of shorter duration with a single average separation of 300 km was regarded as appropriate for initial technique validation. The specific orbit selection was made to enable a repeating ground track over the mission duration with an equatorial separation between the tracks that is commensurate with the desired resolution of the gravity field.

The preceding considerations resulted in the orbit characteristics given in Table 1, namely a simulation duration of 32 sidereal days consisting of 525 revolutions of each satellite. Furthermore, the adopted orbit has the characteristic that the next 525 revolutions would nearly repeat the groundtrack of the simulated 525 revolutions. In addition, the adopted orbits are "frozen" with perigee at 90 degrees as described by *Cook* [1966]. The specific initial conditions for each satellite are given in Table 2.

TECHNIQUES

The primary technique used for the creation of the simulated data was numerical integration of the equations of motion. Extensive studies performed on the characteristics of numerical integration by *Lundberg* [1985], as well as additional supporting studies for the GRM simulation, have demonstrated that truncation error resulting from the adopted numerical integration order and step size would not introduce significant short-period, gravity-like signals in the simulated data, at least for a 36x36 field with an integration period of 32 days. It was not possible to perform the evaluation for

TABLE 1. GRM SIMULATION MODEL

Force Model

Gravitational

$GM = 3.986013 \times 10^{14} m^3 s^{-2}$

$a_e = 6378155$ m

Static: Rapp [private communication, 1985] gravity coefficients complete to 180×180 plus order 0 to 10 coefficients to degree 300

Temporal: None

Luni-Solar: None

Nongravitational

Drag: None

Radiation Pressure: None

(Note: It is assumed that the drag compensation mechanism removes all nongravitational forces.)

Kinematic Models

Earth Orientation

Angular velocity: Constant ($7.29211585531 * 10^{-5}$ rad/sec)

Initial Greenwich mean sidereal time: 1.74731127 radians = 100.1135613°

Polar motion: None

Precession/nutation: None

Orbits

Altitude: 160 km
Inclination: 90 degrees
Eccentricity: 0.00114
Perigee: 90 degrees
Satellite separation: 300 km
Groundtrack repeat period: 32 sidereal days (closure <10 km)
Duration: 32 sidereal days (2,757,250.8 s)

the full gravity field of the simulation; however, one-day studies were performed and are described in the next section. Future studies will be conducted to further investigate this aspect, although it is not expected to produce a significant signal.

To further aid in the control of numerical integration accuracy, the formulation of the differential equations of motion used an Encke-type formulation in which a reference orbit was adopted and the

TABLE 2. INITIAL CONDITIONS FOR SIMULATION*

($t = 0$)

Lead Satellite:	Trailing Satellite:
$x = 0.0$	$x = 0.0$
$y = -150000.0$	$y = 150000.0$
$z = 6514763.771449$	$z = 6514766.990461$
$\dot{x} = 0.0$	$\dot{x} = 0.0$
$\dot{y} = -7817.14687496$	$\dot{y} = -7817.14687496$
$\dot{z} = -179.5130619235$	$\dot{z} = 179.5130619235$

Separation distance = 300000.000017

The initial conditions were provided by Dr. O. Colombo, EG&G Washington Analytical Services. Units are meters for position and meters per second for velocity. The origin of the coordinate system coincides with the earth's center of mass and the coordinate system is nonrotating.

differential equations describe departures from the reference. Studies by *Lundberg* [1985] demonstrated that high numerical accuracy could be achieved for long-term integrations without rectification. In particular, the equations of motion of either satellite are

$$\ddot{\bar{r}} = -\frac{GM\,\bar{r}}{r^3} + \bar{f} \tag{1}$$

where $\bar{r}$ is the geocentric position vector of the satellite expressed in a nonrotating coordinate system, GM is the gravitational parameter of the earth, and $\bar{f}$ is the perturbing force derived from the gradient of the gravitational potential. The Encke procedure uses a reference orbit, $\bar{r}^*$, such that

$$\bar{r} = \bar{r}^* + \bar{\varepsilon} \tag{2}$$

where $\bar{\varepsilon}$ is referred to as the Encke-vector representing the satellite displacement from the reference orbit and described in terms of a nonrotating coordinate system. It follows that

$$\ddot{\bar{\varepsilon}} = -GM\left[\frac{\bar{r}}{r^3} - \frac{\bar{r}^*}{r^{*3}}\right] + \bar{f} - \bar{s} \tag{3}$$

where $\bar{s}$ is the perturbing force on the two-body motion of the reference orbit. The advantage of this formulation is that by properly choosing the reference orbit the Encke-vector would remain much

smaller than $\bar{r}$ (e.g., <1%), thereby resulting in more significant digits in the computation than Eq. (1). The numerical integration parameters used for the simulation are given in Table 3.

TABLE 3. GRM SIMULATION INTEGRATION PARAMETERS

Solution Method

Encke formulation [*Lundberg*, 1985]

Class 2, fixed-mesh, multistep algorithm [*Lundberg*, 1981]

Step Size: 5 seconds

Order: 10

The accuracy of the numerical integration is dependent on the step size and order of the integrator as well as the numerical properties of the computation of the perturbing force, $\bar{f}$. The spherical harmonics formulation was adopted for the computation of the gravitational force because of its well-understood influence on the motion of a satellite (e.g., *Kaula*, 1966). The adopted formulation of spherical harmonics was derived by *Pines* [1973], a formulation with the advantage of retaining a close relationship with the spherical harmonic formulation while eliminating the singularities that exist at the poles with spherical coordinates. Because of the polar orbits used for the mission, the elimination of the singularities was essential. The modified Legendre functions in Pines formulation are computed by recursions in normalized form, hence the normalized spherical harmonic coefficients are used directly. Numerical experiments have been performed with possible recursions by computing the functions to degree and order 300 in 14 decimal digit precision and comparing with 28-digit results. The specific recursion algorithm adopted for the simulation is a column-wise formulation that has demonstrated excellent stability and numerical properties [*Lundberg and Schutz*, 1986]. The Pines formulation code has been further validated by comparison with independent code using the traditional formulation.

In summary, numerical integration was used to obtain the set of simulated data. Each satellite

was treated independently in the process, and the simulated range and range-rate between the satellites were computed from the positions and velocities of the respective satellites. Each satellite's equations of motion were formulated in an Encke-type representation to foster high-accuracy results.

PRELIMINARY RESULTS

Computational experiments were performed in 1983 to provide data from which an estimate of the computer time required for a GRM simulation could be made. This experiment consisted of measurements of the computer time required for the numerical evaluation of a degree and order 180 (180×180) spherical harmonic gravity field. This early evaluation suggested that, while the formulation could be readily adapted to the vectorization environments of modern supercomputers, the time required for a complete simulation would be 10-30 hours; however, the time required on other mainframes would be 1000 hours or more. Further details on these studies with a variety of computers are given by *Schutz* [1986].

Preliminary simulation results for initial test and evaluation purposes were computed using a one-day interval of time. These results were obtained using a Cray X-MP/48 and an Amdahl 1200. The results from the two machines agreed to 13 decimal digits at the end of the integration period. The execution of the same code required 1634 seconds on the Amdahl 1200 and 1575 seconds on the Cray X-MP using a single processor. Furthermore, the Fortran compilers of both machines automatically vectorized the same loops in the code and both identified the recursive algorithms used in the computation of the modified Legendre functions as an area requiring special treatment for vectorization.

The one-day preliminary results were compared with an integration performed using the simulation gravity field but truncated at degree and order 36. The initial conditions in Table 2 were used, and the computations with the 36×36 field were performed using a Cyber 170/750. The Cray X-MP result with the Table 1 model was used to compute the instantaneous range and range-rate between

the satellites, from which the range and range-rate computed from the 36x36 field was subtracted. The instantaneous range vector, $\bar{\rho}$, is computed as

$$\bar{\rho} = \bar{r}_L - \bar{r}_T \tag{4}$$

and the range is $\rho = [\bar{\rho} \cdot \bar{\rho}]^{1/2}$, where $\bar{r}_T$ is the position vector of the trailing satellite and $\bar{r}_L$ refers to the leading satellite. The instantaneous range-rate, $\dot{\rho}$, is

$$\dot{\rho} = \frac{\bar{\rho} \cdot \dot{\bar{\rho}}}{\rho} \tag{5}$$

The resulting differences, or residuals, in range ($\Delta\rho$) and range-rate ($\Delta\dot{\rho}$) computed with the respective ephemerides are shown in Figures 1 through 3. The range and range-rate residuals for the first day are shown in Figures 1 and 2. The range-rate residuals are shown in Figure 3 for the first 10,000 seconds to enhance the illustration of small amplitude signals that exist in the simulated data.

Various experiments were performed to further vectorize the code in order to reduce the execution time. Of particular importance were the implementation of procedures for vectorizing the recursive computation of the Legendre functions, achieved by computing all the elements parallel to the diagonal in a vector operation. Experiments showed that this procedure reduced the execution time required for the overall gravity computation by more than a factor of two. In the following discussions on the final results, this vectorized computation of the Legendre functions by recursions was used.

In addition to the computational speed, the precision of various machines is of importance. Computational precision is dependent on the number of bits allocated to storage of the floating point mantissa and on the central processor design which includes hardware rounding operations. The mantissa bit allocation for the Amdahl 1200 is 56 bits and the Cray X-MP is 48 bits. Although the roundoff error of the Amdahl 1200 is about 10^{-15} and about 10^{-14} on the Cray X-MP, effective hardware accuracy guards are provided on the Cray computer to assist in the control of roundoff

error. Experiments by the authors on various problems, including unstable dynamical systems that exhibit significant response to roundoff error, has shown these guards to be effective. Such accuracy guards were invoked in all computations using the Cray X-MP described in this report.

SIMULATION RESULTS

The simulation results for the full 32-day period were performed using a Cray X-MP/216 computer with a time grant from Cray Research, Incorporated (CRI). The machine was located at the CRI Mendota Heights, Minnesota, facility and the computations were performed in November 1985 using a block of dedicated machine time. A subsequent verification test was performed on the Cray X-MP/24 installed at the University of Texas System Center for High Performance Computing in March 1986. The central processor time required on the Mendota Heights machine was 6 hours 28 minutes. Furthermore, comparison with the earlier results illustrates that the vectorization of the Legendre recursion substantially influenced the overall computation time. Other analyses have shown that the gravity force evaluation consumed more than 90% of the computation time.

The accuracy associated with the integration step size of 5 seconds was evaluated by comparison with an integration performed with a 2.5-second step size. However, the integration was performed for one day since the full 32-day computation was estimated to require about 13 hours for a step size of 2.5 seconds. The difference between the range and range-rate computed with the different step sizes are shown in Figures 4 and 5.

The effect of step size on the range between the two satellites is illustrated in Figure 4. Over the one day interval, the effect is less than ten microns. More importantly, the periodic effect has an amplitude of about 3 microns at a frequency of one cycle per orbital revolution. Similarly, the step size influence on range-rate is shown in Figure 5 with a peak of less than 0.3 microns per second, but with a root mean square of less than 0.1 microns per second and no evidence of a linear trend in the differences. Consequently, it can be tentatively concluded that the 5-second step size does not

adversely influence the results at a level exceeding the anticipated measurement precision. Nevertheless, plans are being made to completely verify this conclusion through computations for the entire 32 days.

The state vectors of each satellite after 32 sidereal days are given in Table 4 for the nearest integration node point, which differs from the exact 32 sidereal day time by 0.8 seconds. Comparison with Table 2 shows that the y-components have the largest difference, about 5400 m for the lead satellite and 2300 m for the trailing satellite. Extrapolating the position forward in time to account for the 0.8-second effect results in a smaller difference for the lead satellite but a larger one for the trailing satellite. In either case, a closure to less than 10 km appears to have been achieved.

TABLE 4. FINAL CONDITIONS FOR SIMULATION

(Time = 2757250.0 seconds)

Lead Satellite:	Trailing Satellite:
$x = -25.5702759$	$x = 28.7872855$
$y = -144635.9583872$	$y = 152283.2962437$
$z = 651517.4216461$	$z = 6514295.7534658$
$\dot{x} = -1.4053666402$	$\dot{x} = -1.4535883592$
$\dot{y} = -7817.7289670476$	$\dot{y} = -7817.5867963785$
$\dot{z} = -173.1909583647$	$\dot{z} = 182.1378972218$

Separation distance = 296919.342351

Units are meters for position and meters per second for velocity.

The time histories of the instantaneous range and range-rate for the complete 32-day simulation period are shown in Figures 6 and 7. The range illustrated in Figure 6 exhibits a short period (orbital period) with an amplitude of 450 m. Long period effects are evident also, due possibly to resonances, as well as indications that the satellites begin a linear drift at about 16 days. The range-rate in Figure 7 exhibits essentially a zero mean with a short period amplitude of about 0.8 m s^{-1}.

Since one of the primary purposes of the GRM is to measure the gravity field, it is reasonable to expect that the field available at GRM launch for data analysis will be in error. Based on the planned

TRANET tracking system, these ground-based data would be used to determine an orbit that fit the data in accordance with some criteria, such as least squares. To simulate this process, the ephemerides generated on the Cray X-MP with the Table 1 model were used as "observations" to an estimation process that determined epoch position and velocity of the respective satellites. In this estimation process, however, the reference gravity field differed from the Table 1 field.

Two reference fields have been used in the investigation. In the first case, the influence of high degree and order coefficients was investigated by truncating the Table 1 field at degree and order 36. Consequently, this case used the "true" coefficients for the 36x36 portion of the field, but mismodeled all coefficients of degree and order greater than 36 by effectively setting those coefficients to zero. In the second case, the reference field was GEM-10B [*Lerch et al.*, 1981] which results in a mismodeling of all coefficients, including zero values for coefficients of degree and order exceeding 36. In both cases, the initial position and velocity vectors (six parameters) and a constant along-track force parameter were estimated. The latter parameter was used to remove any inherent numerical integration differences, however, the estimated quantity was small and approaching the level of computational precision indicating close compatibility between the full model integration and the reference model integration.

The ephemerides resulting from the estimation using the truncated (36x36) Table 1 reference field were compared to the full model (Table 1) ephemerides. The position differences over 32 days result in position residuals with an overall RMS of 949 m for the leading satellite and 904 m for the trailing satellite. These differences for the leading satellite, resolved into radial, along-track and cross-track components, are shown in Figures 8, 9 and 10, respectively. Similar characteristics are exhibited by the trailing satellite. The longest period variation in the along-track component is conjectured to be associated with the odd-degree zonal harmonics, while the approximately six-day period is believed to be due to resonant coefficients. Experiments with the second case, the GEM-

10B field, show position residuals with an RMS of 950 m for the leading satellite and 907 m for the trailing satellite, as illustrated in Figures 11, 12 and 13. Because of the general similarity between these two cases, it is apparent that the coefficients of degree and order greater than 36 have significant orbit perturbation influence on the low altitude GRM. This behavior will have some bearing on the orbit determination accuracy requirement of 300 m [*Keating et al.*, 1986].

Range and range-rate residuals were computed using the Cray ephemerides resulting from the integration with the Table 1 model and the GEM-10B ephemerides fit to the Cray result. The range residuals are given in Figure 14, and the range-rate residuals are in Figure 15. Since the linear trend apparent in Figure 6 has either been removed or diminished, it can be concluded that the drift is primarily the result of the adopted orbit characteristics and the low degree and order coefficients. In general, a rich spectrum of frequencies appears to exist in Figures 14 and 15 that will provide a useful basis for further analysis, especially in the application of techniques designed to recover the gravity field from such data.

RECOMMENDATIONS

This report has described the results of the first simulation of a GRM with emphasis on the gravitational aspects. The simulation model has been chosen to enhance the gravitational signal for the testing and validation of gravity recovery techniques. The results of the simulation are available for further analysis on a high density (6250 cpi) magnetic tape.

Based on the results described in this report, several recommendations for future study can be made as follows:

- The orbit determination accuracy will be significantly influenced by a priori errors in the gravity field, including coefficients exceeding degree and order 36; consequently techniques should be investigated that reduce the influence of the resulting orbit errors on the GRM gravity field recovery.

- A more realistic simulation of the TRANET tracking distribution should be investigated directed toward the influence on the range-rate residuals.
- Examination of alternate tracking systems, such as satellite-borne Global Positioning System receivers should be performed.
- Implementation of more realistic force models, especially tide models, and kinematic models, especially those describing the orientation of the earth in space.
- Simulation of outer satellite drag and creation of a set of range and range-rate simulated data that include thrusts associated with a drag compensation mechanism.
- Investigation of the influence of time-varying features in the ocean surface on the range and range-rate.
- Further investigation of the numerical precision associated with the simulation.
- Examination of the influence of satellite separation and altitude.

Efforts to investigate these GRM aspects are in progress.

ACKNOWLEDGMENTS

This research has been supported by the National Aeronautics and Space Administration under Grant No. NAG5-528. Computer time for the final results of this study was provided by Cray Research, Incorporated (CRI). The individual contributions of J. Padian, W. Eue and C. Hsiung of CRI are gratefully acknowledged. Computer time for preliminary studies was provided by Amdahl Corporation, and the assistance of A. Tait was very helpful.

REFERENCES

Colombo, O. C., The global mapping of gravity with two satellites, *Netherlands Geodetic Commission, 7* (3), 1984.

Cook, G. E., Perturbations of near-circular orbits by the earth's gravitational potential, *Planet. Space*

Sci., 14 433-444, 1966.

Kaula, W. M., *Satellite Geodesy*, Blaisdell Co., Waltham, Mass., 1966.

Kaula, W. M., Inference of variations in the gravity field from satellite-to-satellite range rate, *J. Geophys. Res., 88* (B10), 8345-8349, 1983.

Keating, T., P. Taylor, W. Kahn, and F. Lerch, Geopotential research mission: Science, engineering and program summary, *NASA Technical Memorandum 86240*, May 1986.

Lerch, F. J., B. H. Putney, C. A. Wagner, and S. M. Klosko, Goddard earth models for oceanographic applications (GEM 10B and 10C), *Mar. Geod., 5* (2), 145-187, 1981.

Lerch, F. J., S. M. Klosko, G. B. Patel, and C. A. Wagner, A gravity model for crustal dynamics (GEM-L2), *J. Geophys. Res., 90* (B11), 9301-9311, 1985.

Lundberg, J. B., Numerical integration techniques for satellite orbits, Center for Space Research, The University of Texas at Austin, May 1981.

Lundberg, J. B., Computational errors and their control in the determination of satellite orbits, *CSR-85-3*, Center for Space Research, The University of Texas at Austin, March 1985.

Lundberg, J. B., and B. E. Schutz, Recursion formulas of Legendre functions for use with non-singular geopotential models, In preparation, 1986.

National Research Council, *Applications of a Dedicated Gravitational Satellite Mission*, Washington, D. C., 1979.

Pines, S., Uniform representation of the gravitational potential and its derivatives, *AIAA J., 11* (11), 1508-1511, November 1973.

Rapp, R. H., The earth's gravity field to degree and order 180 using Seasat altimeter data, terrestrial gravity data, and other data, *Geodetic Science Rep. No. 322*, Ohio State University, December 1981.

Schutz, B. E., Supercomputers and Satellite Geodesy, Center for Space Research, The University of Texas at Austin, 1986.

Taylor, P. T., T. Keating, W. D. Kahn, R. A. Langel, D. E. Smith, and C. C. Schnetzler, GRM: Observing the terrestrial gravity and magnetic fields in the 1990's, *Eos Trans. AGU, 64* (43), 609-611, Oct. 25, 1984.

Wagner, C. A., Direct determination of gravitational harmonics from low-low GRAVSAT data, *J. Geophys. Res., 88* (B12), 10309-10322, 1983.

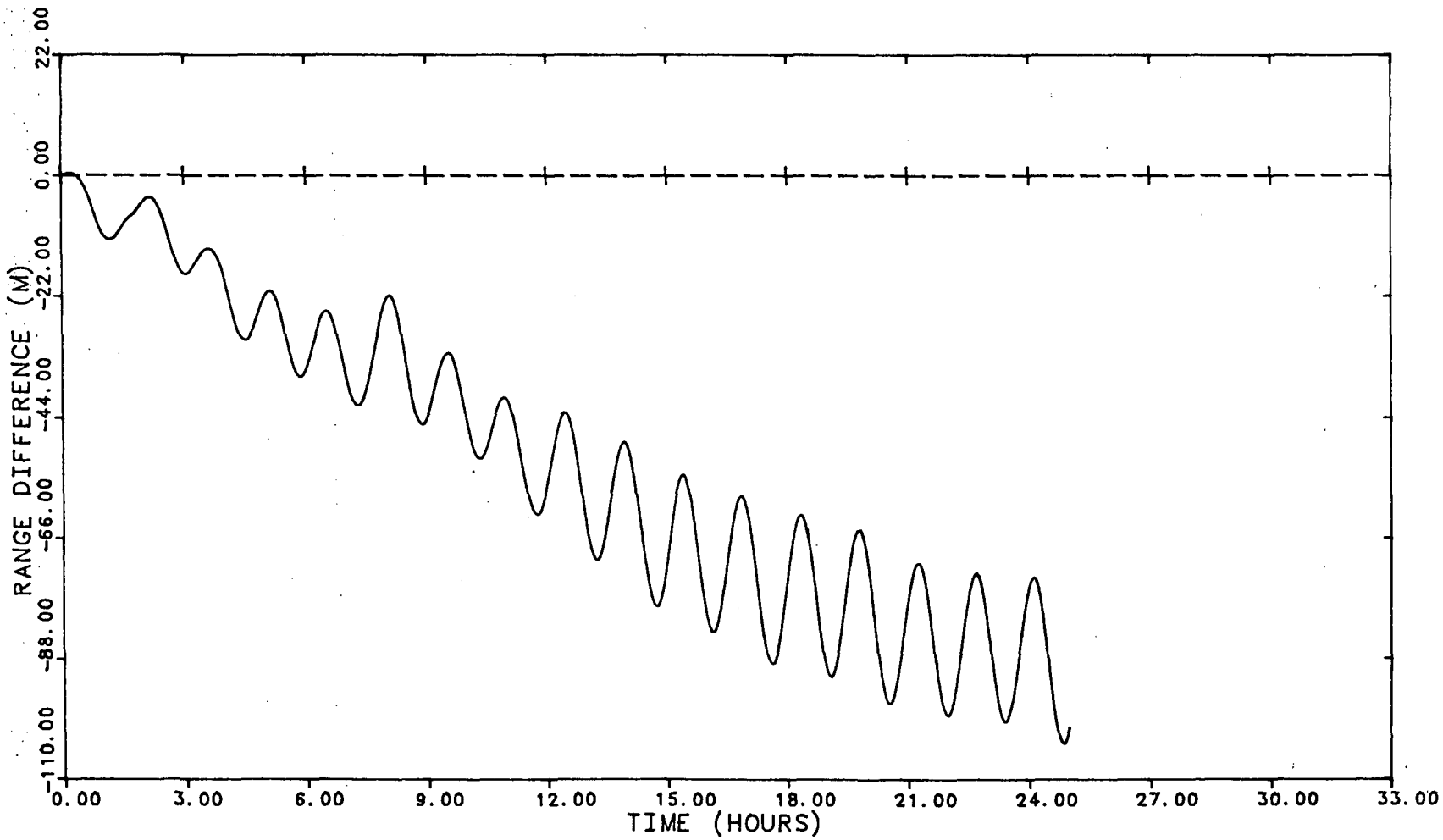

Figure 1. Range residual (full model minus 36×36 model) for one day (plotted every 45 seconds)

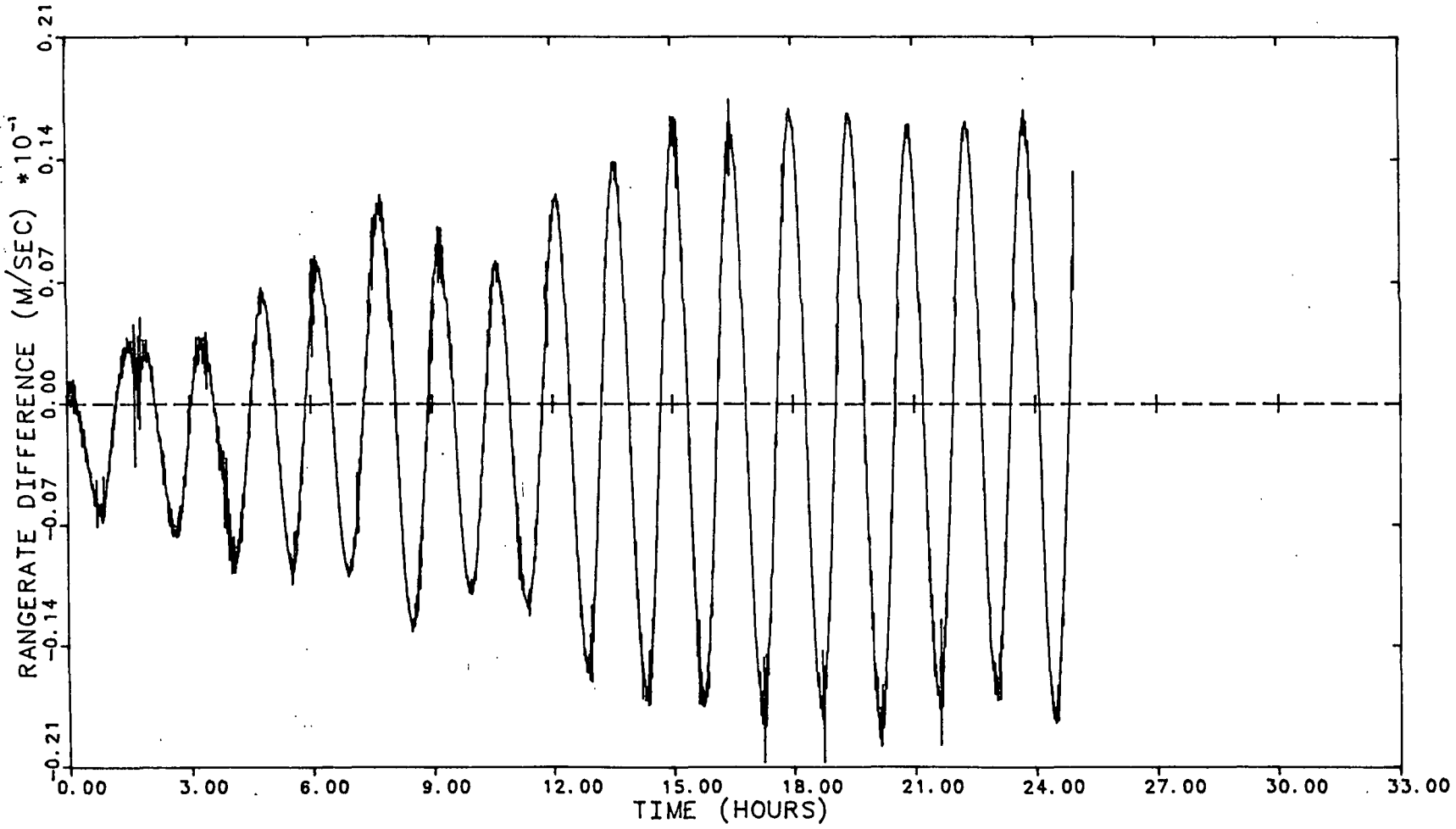

Figure 2. Range-rate residual (full model minus 36x36 model) for one day (plotted every 45 seconds)

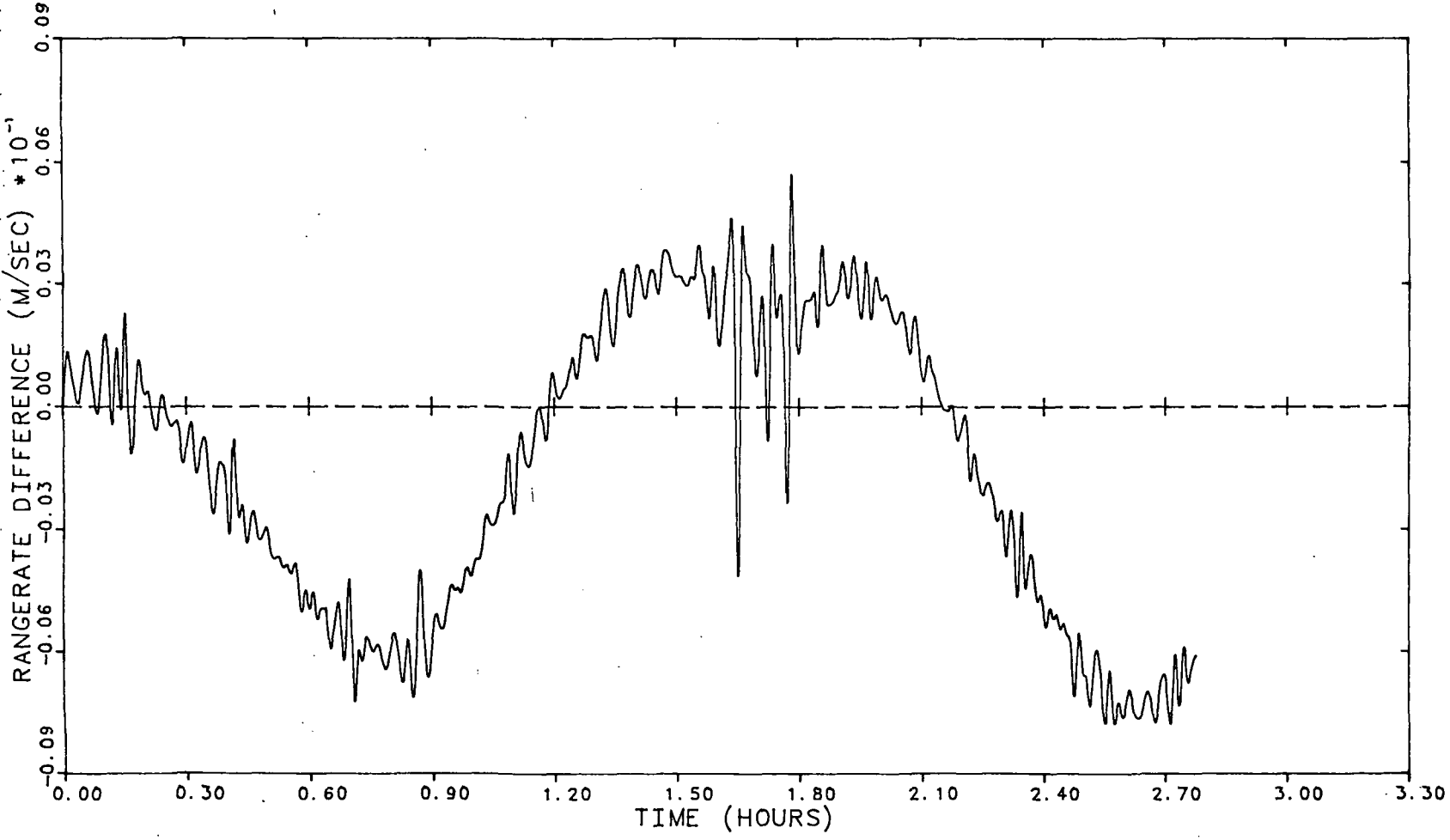

Figure 3. Range-rate residual (full model minus 36x36 model) for 10,000 seconds (plotted every 5 seconds)

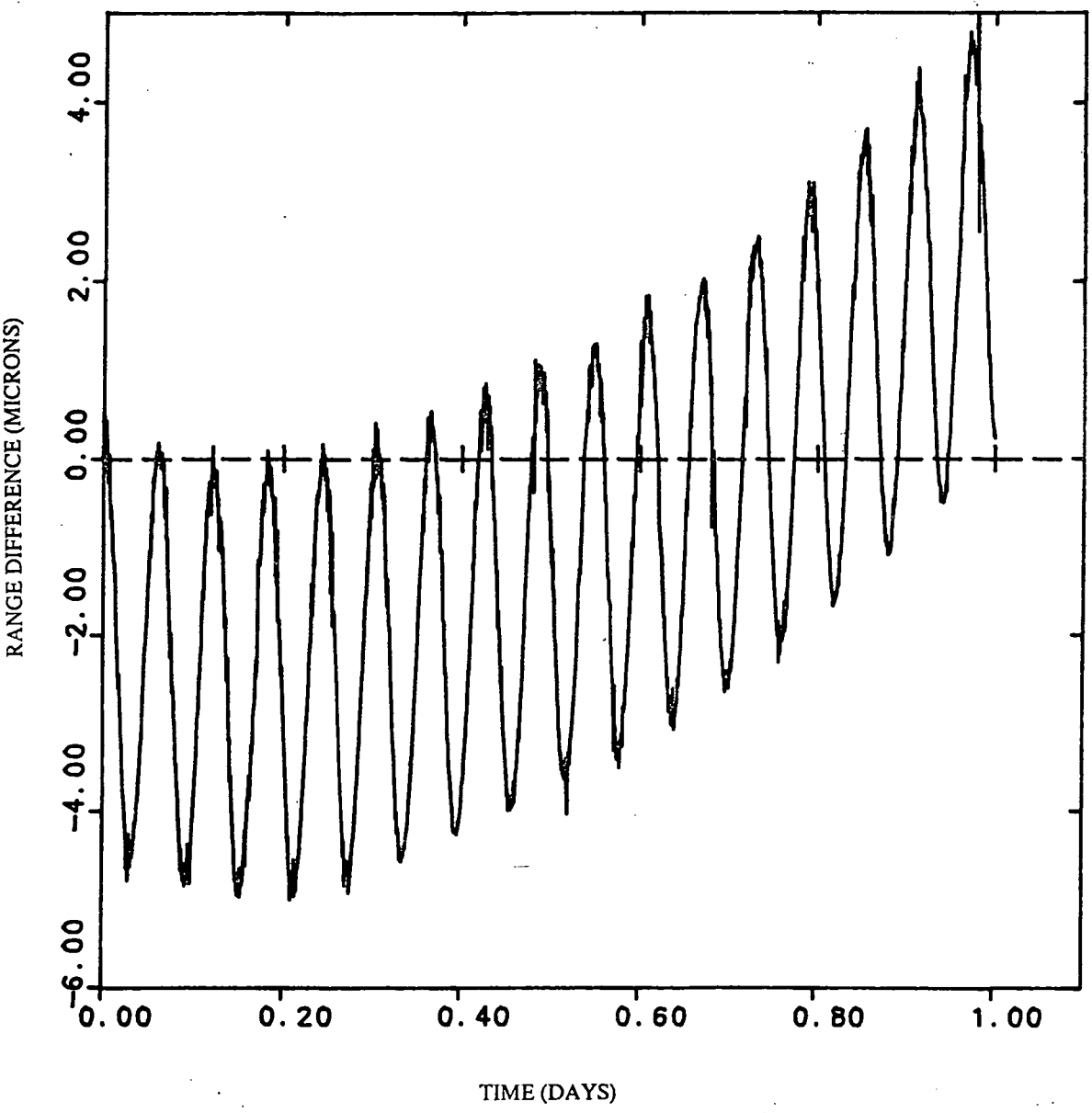

Figure 4. Range residuals, 5-second minus 2.5-second step sizes, full model for one day

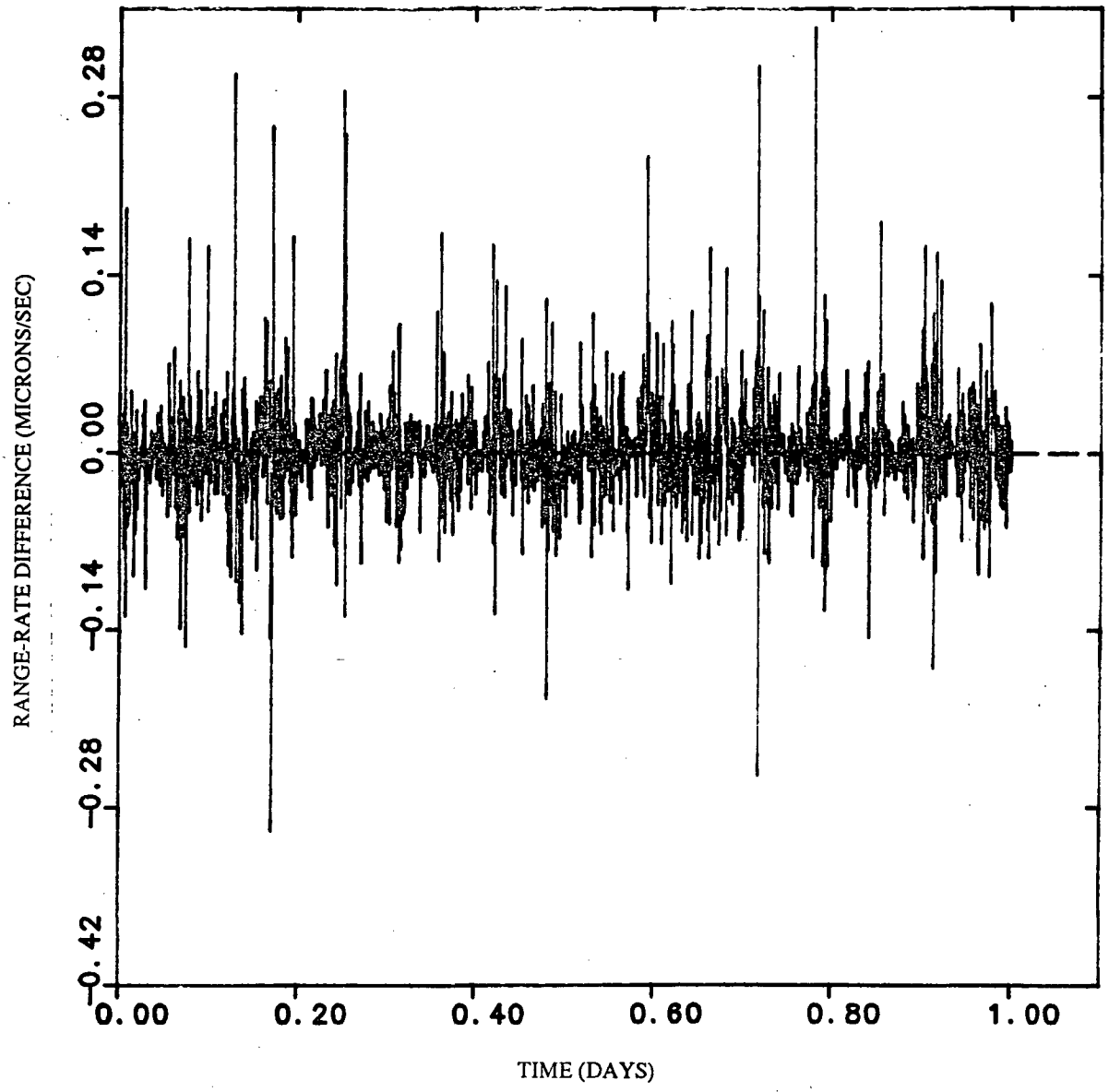

Figure 5. Range-rate residuals, 5-second minus 2.5-second step sizes, full model for one day

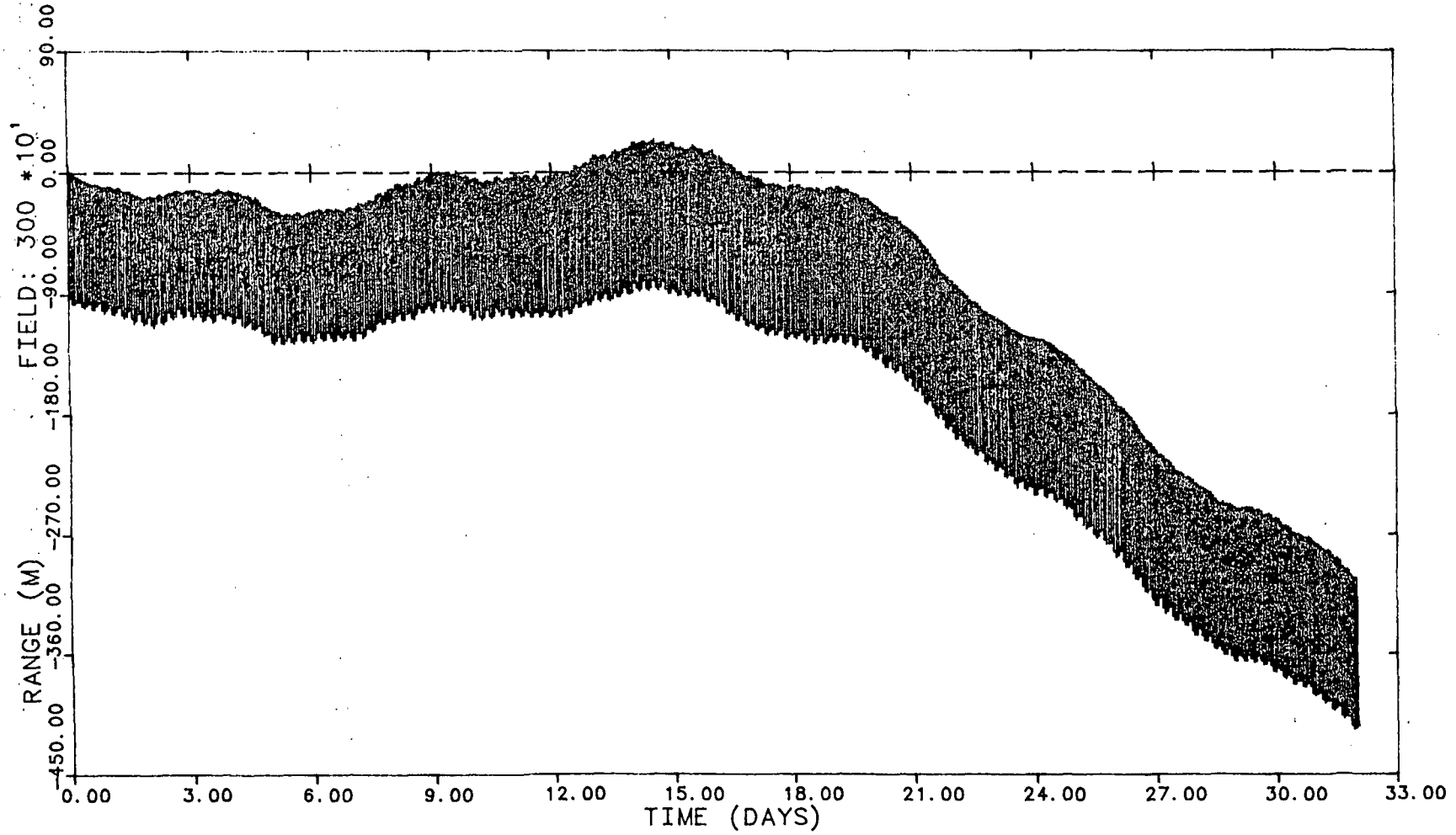

Figure 6. Range history for Table 1 model

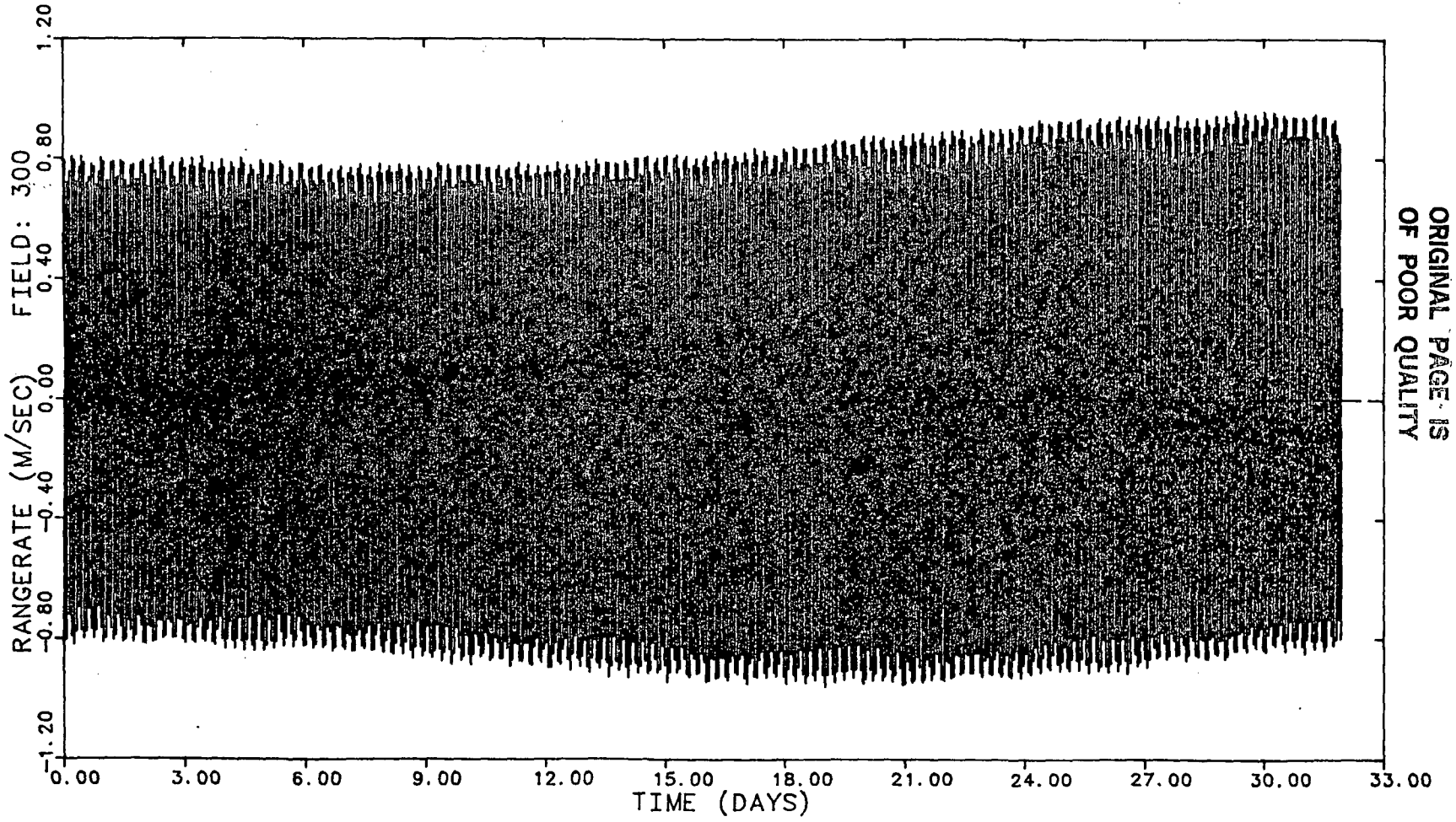

Figure 7. Range-rate history for Table 1 model

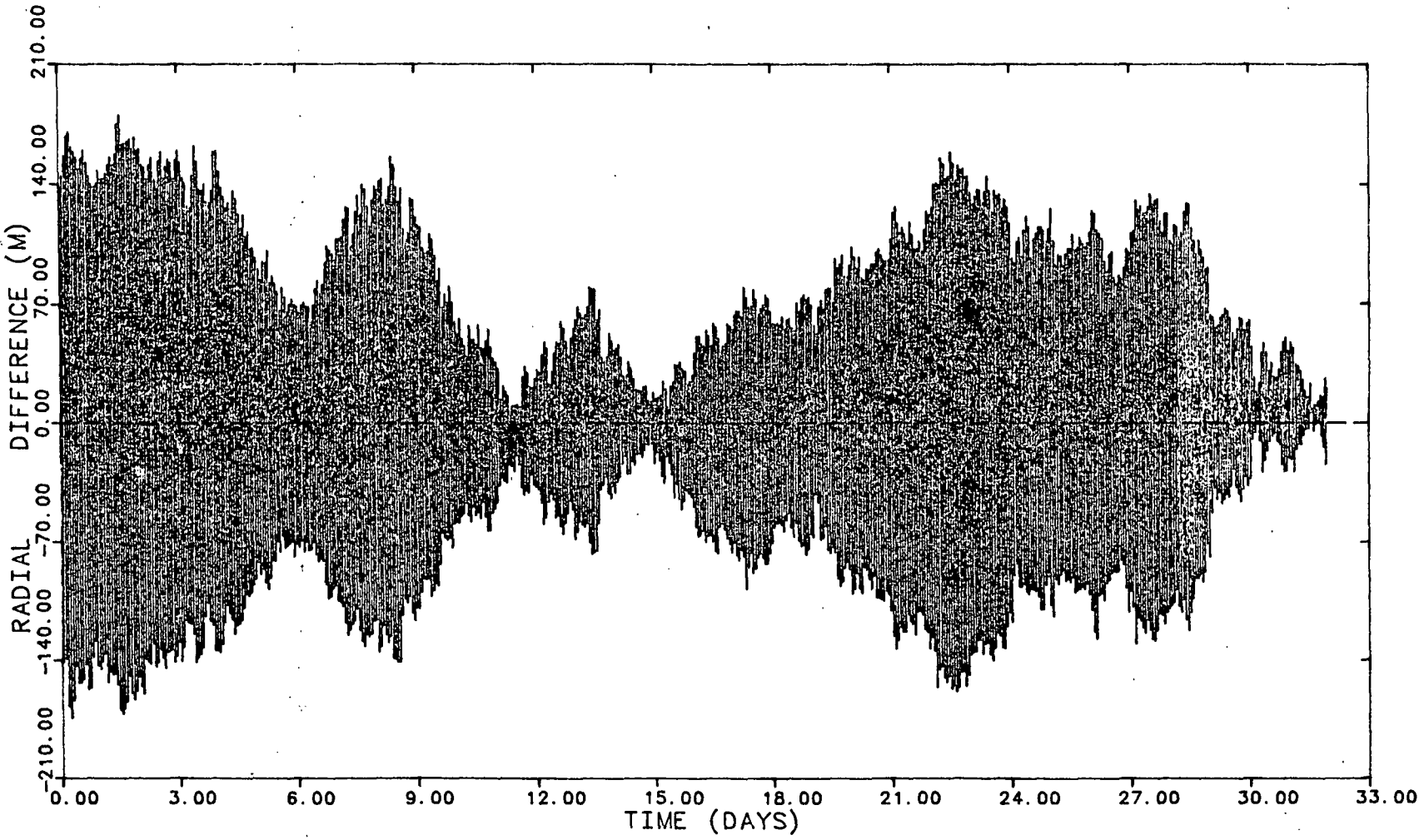

Figure 8. Radial ephemeris differences for lead satellite (36x36 Table 1 model minus full model)

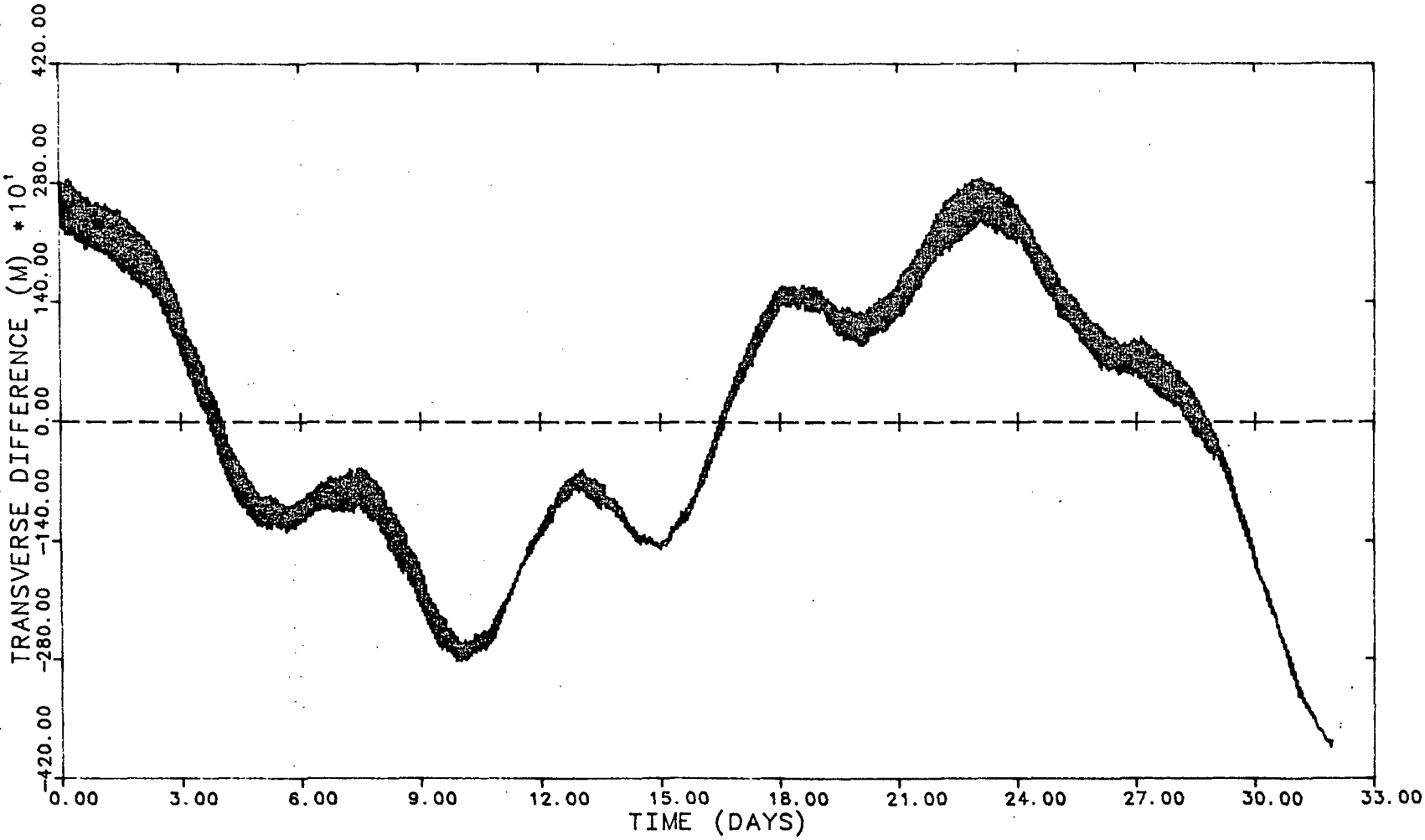

Figure 9. Along-track ephemeris differences for lead satellite (36x36 Table 1 model minus full model)

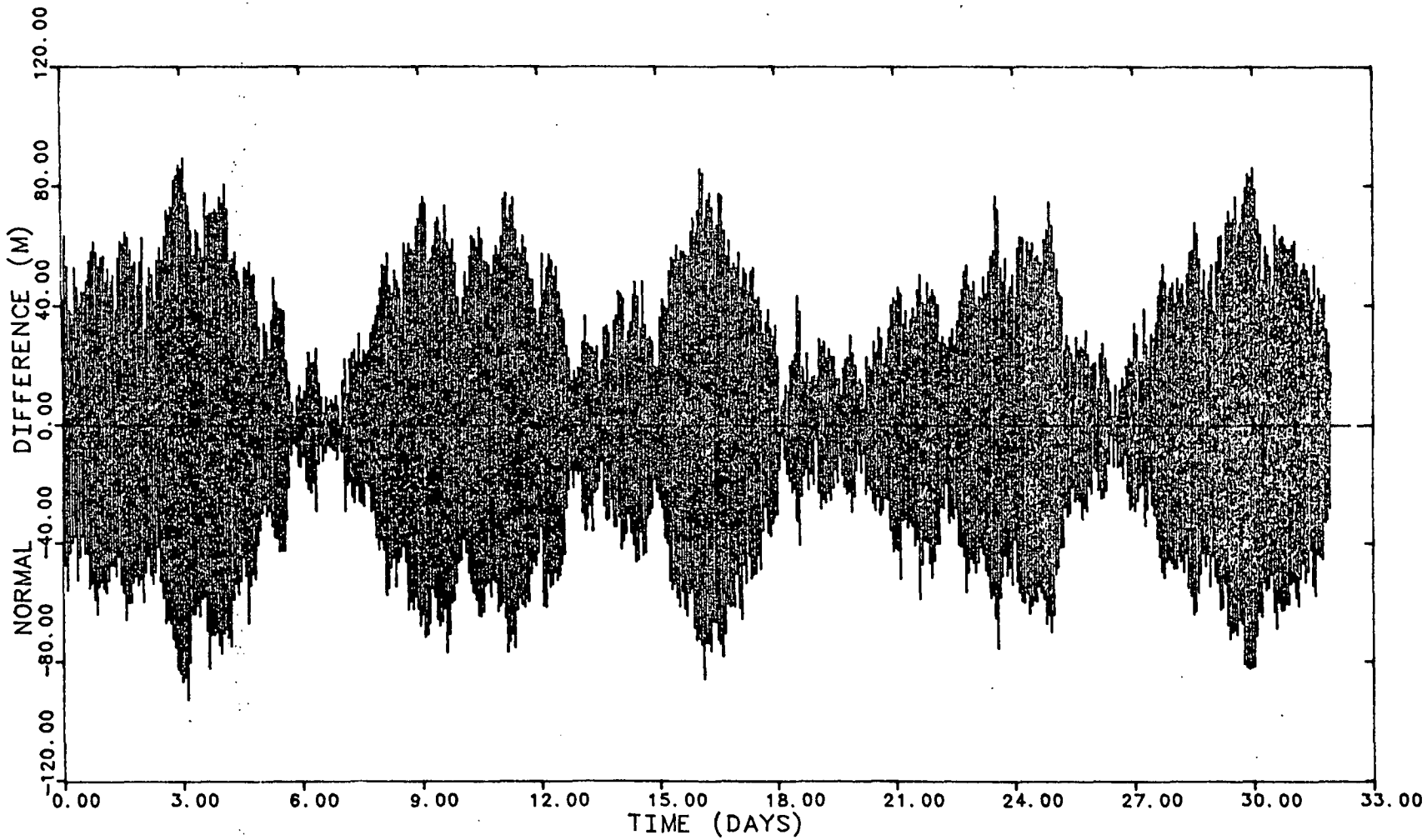

Figure 10. Cross-track ephemeris differences for lead satellite (36×36 Table 1 model minus full model)

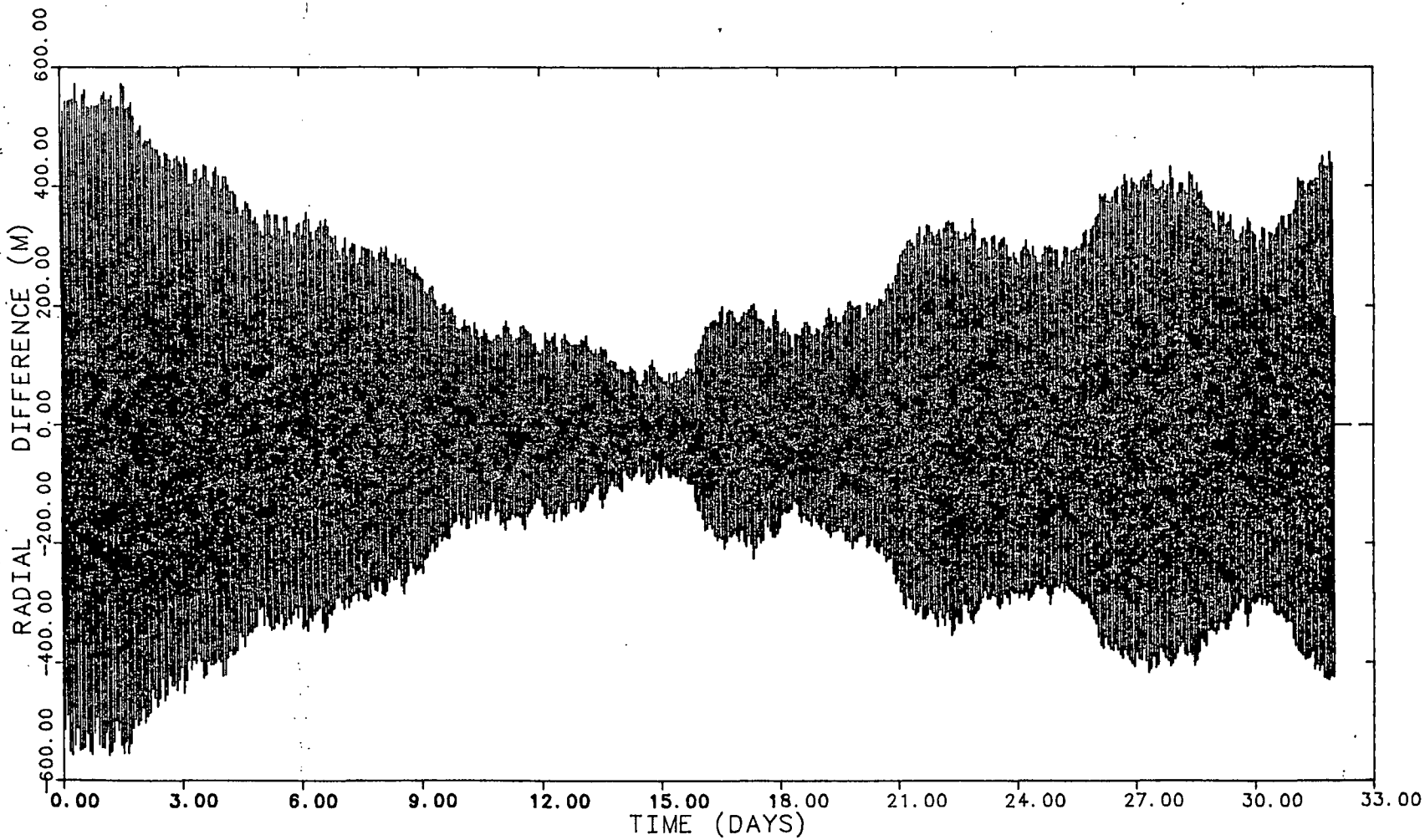

Figure 11. Radial ephemeris differences for lead satellite (GEM-10B minus Table 1 model)

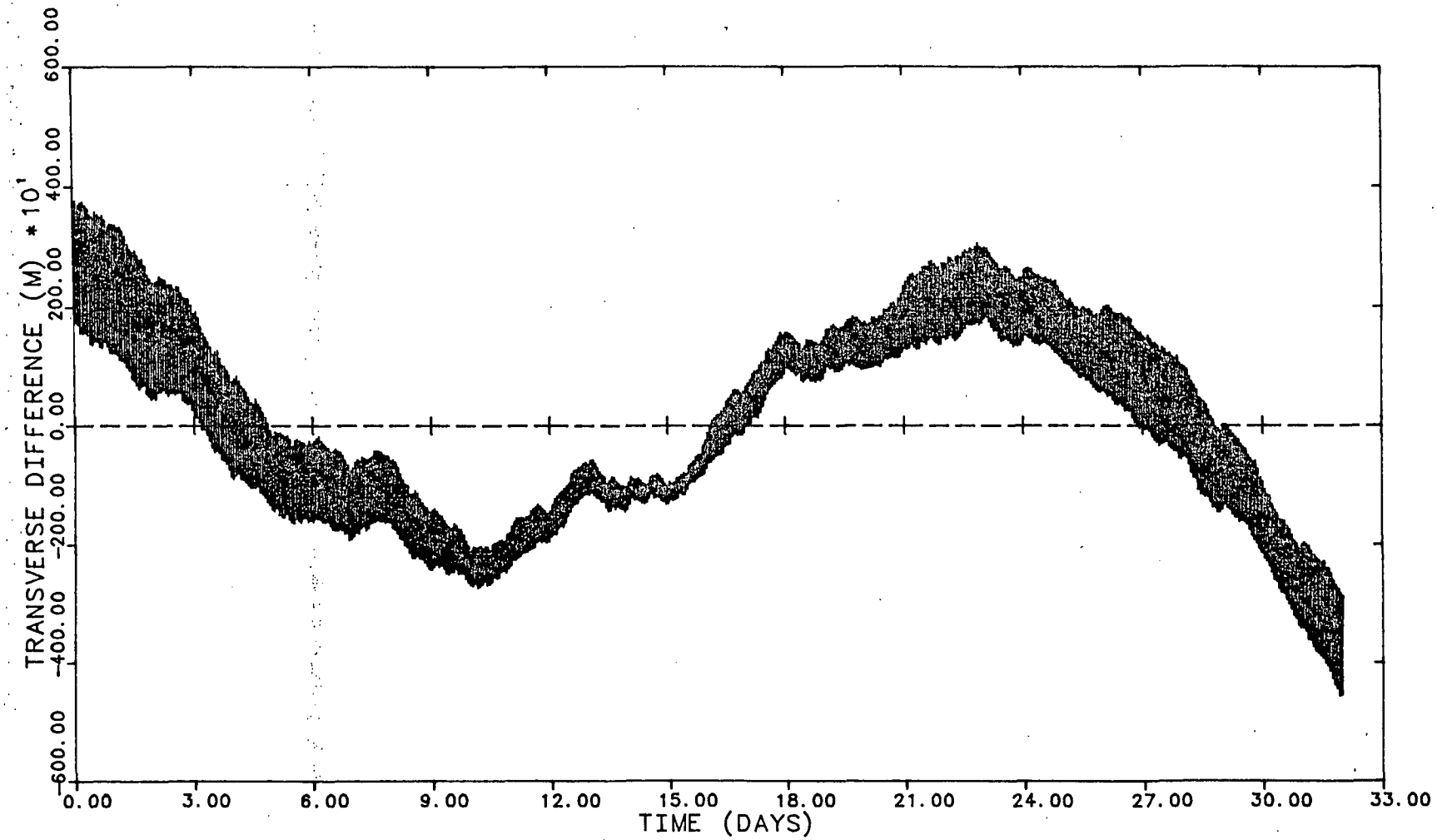

Figure 12. Along-track ephemeris differences for lead satellite (GEM-10B minus Table 1 model)

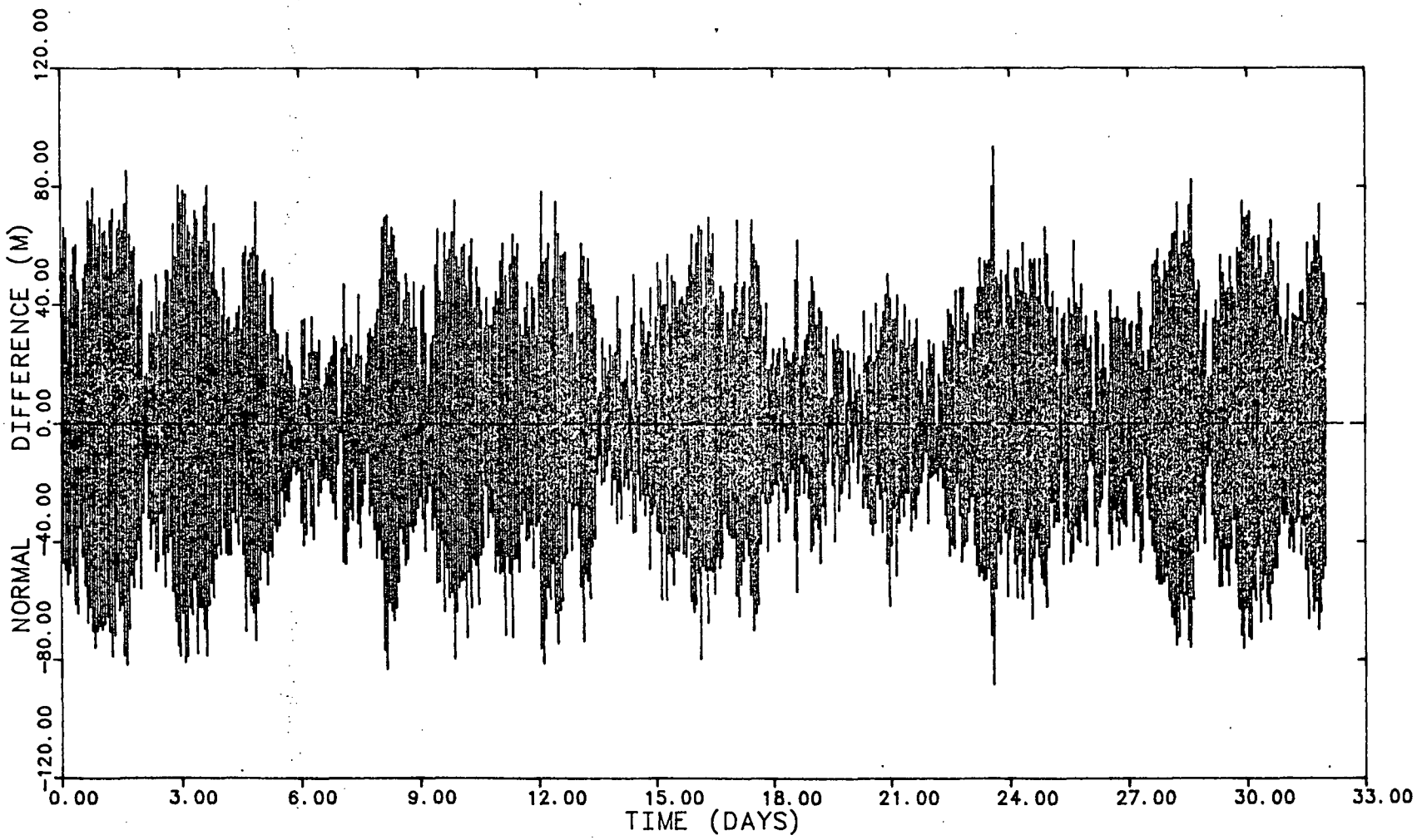

Figure 13. Cross-track ephemeris differences for lead satellite (GEM-10B minus Table 1 model)

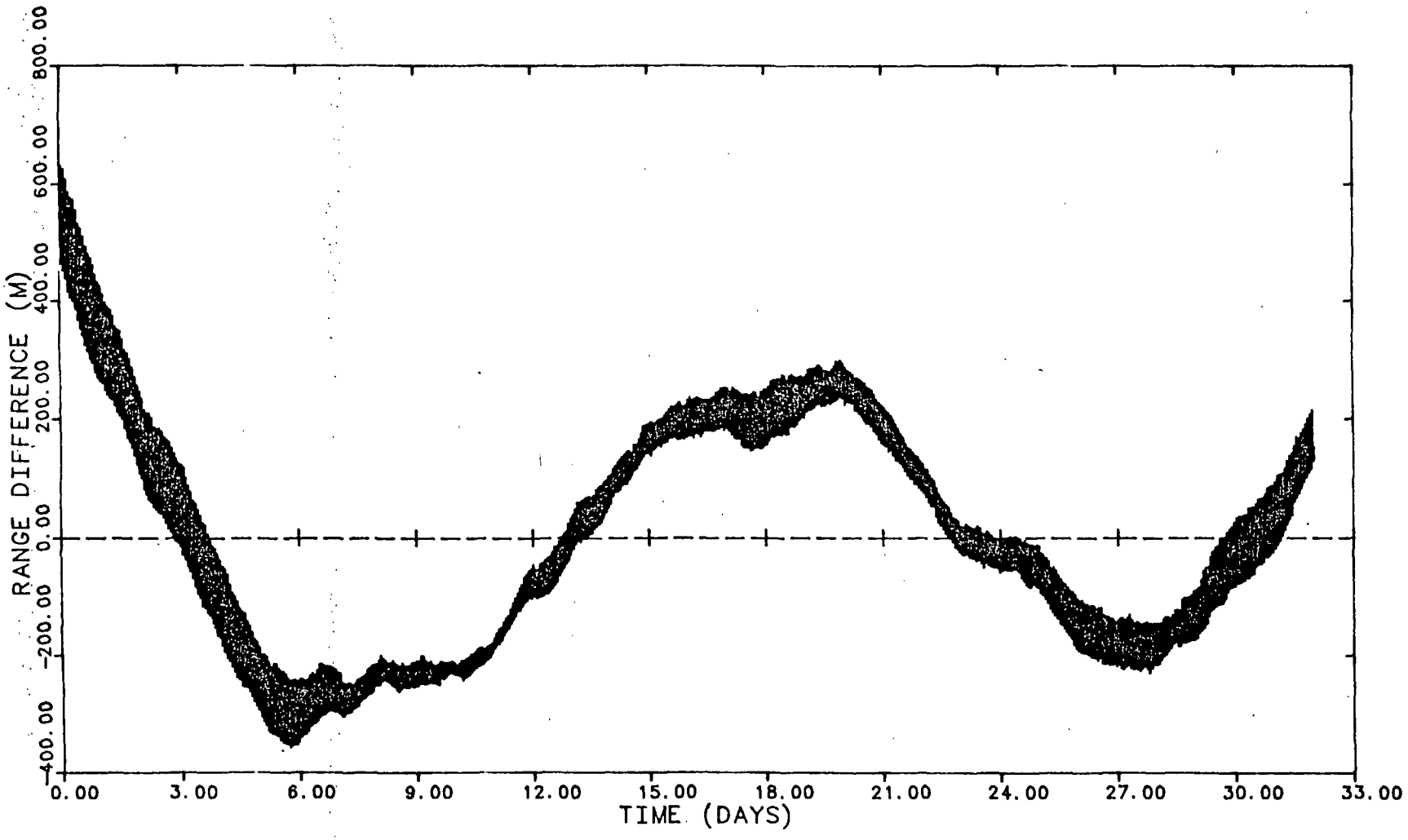

Figure 14. Range residual (Table 1 model minus GEM-10B ephemeris)

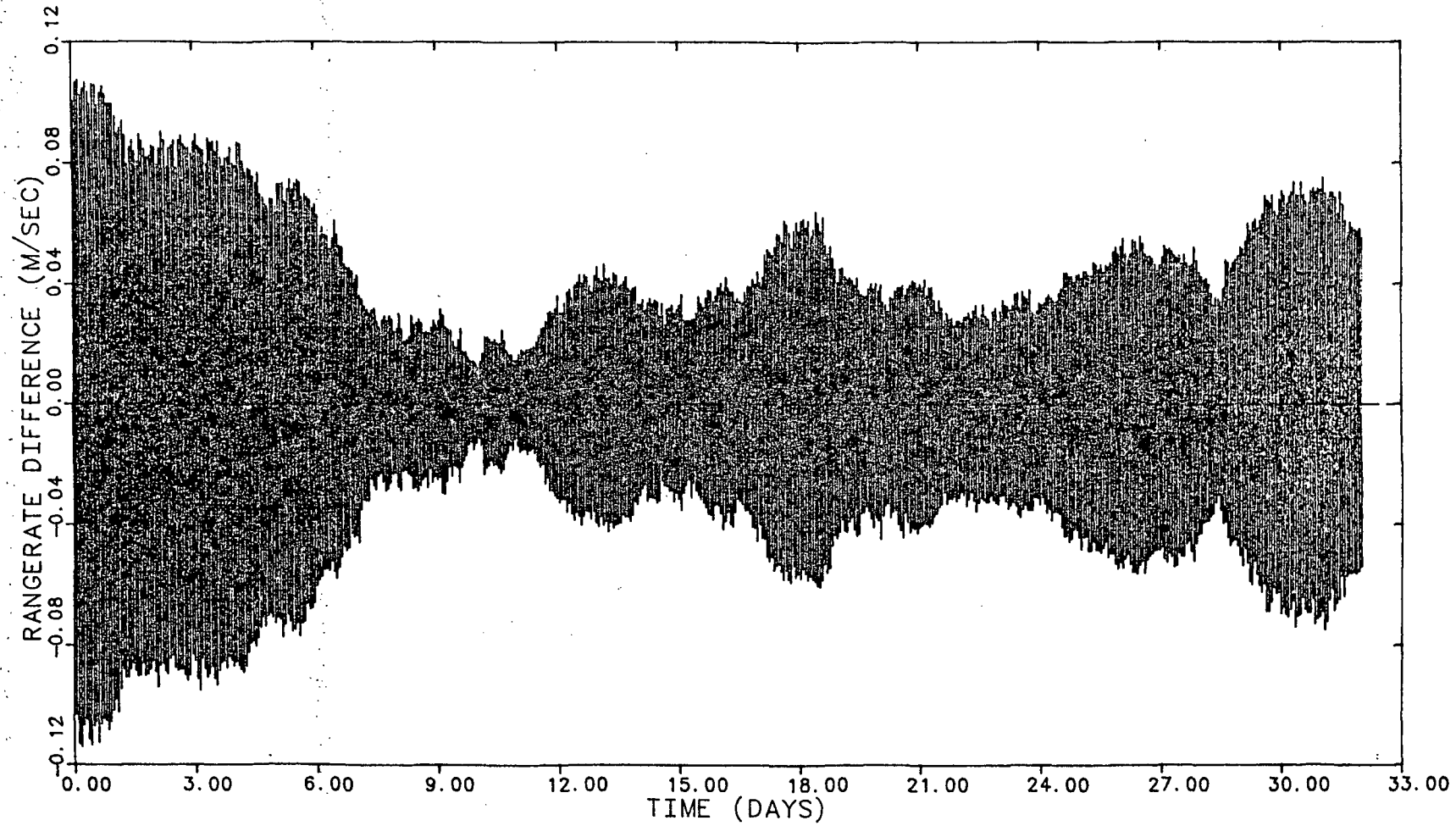

Figure 15. Range-rate residual (Table 1 model minus GEM-10B ephemeris)

APPENDIX B

DISTRIBUTION FORMAT

Center for Space Research
The University of Texas at Austin
May 2, 1986

GRM SIMULATION: SGRM8511

Distribution Format

Characters per record:	80
Records per block:	300
Characters per block:	24000
Character set:	either ASCII or EBCDIC (as noted on label)
Density:	6250 cpi

There are three files on the tape:

File #1: Contains the time, range, and range-rate from the GRM simulation using the OSU322 gravity (180×180 and orders 0 to 10 for degrees 181 to 300). Also contains the ephemerides for a reference orbit fit to the GRM simulation using the modified GEM-10B geopotential.

File #2: OSU322 gravity file.

File #3: GEM-10B gravity file, with modified GM and a_e

The formats for reading files 2 and 3 are at the beginning for each file. The format and data content for the first file is as follows:

Data at each time point:

t_i time tag in seconds from the start of the ephemeris at $t = 0$.

ρ_i observed range between the two satellites (noiseless)

$\dot{\rho}_i$ observed range-rate between the two satellites (noiseless)

η_i * measurement noise parameter

$\bar{r}_1$ ** position vector of the lead satellite for the 36×36 reference orbit

$\bar{v}_1$ ** velocity vector of the lead satellite for the 36×36 reference orbit

$\bar{r}_2$ ** position vector of the trailing satellite for the 36×36 reference orbit

$\bar{v}_2$ ** velocity vector of the trailing satellite for the 36×36 reference orbit

* The measurement noise parameter ranges from −5.0 to +5.0 and has a Gaussian distribution. Scaling this quantity by the standard error of the measurement precision enables noise to be added to the observations. For example, to create a range-rate observation with noise, $\tilde{\dot{\rho}}_i$, $\tilde{\dot{\rho}}_i = \dot{\rho}_i + \sigma\eta_i$, where σ might be 0.000001 m s^{-1}.

** These data are expressed in an earth-fixed, rotating coordinate system. The position and velocity vectors were transformed from the nonrotating, inertial coordinate system of integration to the earth-fixed system using the same transformation matrix, i.e.,

$$\bar{r}_i = [R]\,\bar{r}_{I_i}$$

$$\bar{v}_i = [R]\,\bar{v}_{I_i}$$

where $\bar{r}_{I_i}$ and $\bar{v}_{I_i}$ are the position and velocity vectors in inertial coordinates and $[R]$ is the transformation matrix between the nonrotating, inertial system and the earth-fixed, rotating system.

Three records (card images) are used to display the data at each time point; the card images and formats are:

Record No. k	t_i	ρ_i	$\dot{\rho}_i$	η_i	x_1	y_1
	F9.1	F18.10	F14.11	F7.4	F16.7	F16.7
Record No. $k+1$	z_1	$\dot{x}_1$	$\dot{y}_1$	$\dot{z}_1$	x_2	
	F16.7	F16.10	F16.10	F16.10	F16.7	
Record No. $k+2$	y_2	z_2	$\dot{x}_2$	$\dot{y}_2$	$\dot{z}_2$	
	F16.7	F16.7	F16.10	F16.10	F16.10	

The ground tracks of the satellites nearly repeat after 32 sidereal days (2757250.8 sec); the data stored on the magnetic tape span 32 mean solar days (2764800 sec).